Chapter 4 Pre-treatment of petroleum refinery wastewater by coagulation and flocculation using mixed coagulant: optimization of process parameters using response surface methodology (RSM)

Abstract

The present work reports the efficacy of three coagulants $CuSO_4$, $FeCl_3$, and $CuSO_4$+$FeCl_3$ (both salt mixed in 1:1 ratio (v/v)) for the treatment of wastewater from effluent treatment plant of petroleum refinery using coagulation and flocculation process. The independent parameters such as pH and dosage of coagulants were optimized using response surface methodology with central composite design technique considering final pH, reduction in COD, turbidity, TDS, and color as dependent variables. The statistical fitness of the developed model was checked using ANOVA. A second-order quadratic model (R^2> 95 %) was best fitted to develop the relationship between independent and dependent variables. Charge neutralization, sweep flocculation, adsorption, and formation of tribasic copper chloride (TBCC) were mainly responsible for coagulation and flocculation processes. Results showed that mixed coagulant $CuSO_4$+$FeCl_3$ delivered a better result than $CuSO_4$ and $FeCl_3$ individually. $CuSO_4$+$FeCl_3$ along with adsorption and sweep flocculation, forms tribasic copper chloride (TBCC) as a proceeding intermediate in the pH range 5-7. The TBCC formation enhanced the flocculation by destabilizing colloidal and suspended particles due to its catalytic, decolorizing, and octahedral

structural properties. Maximum reduction in COD (76.77 %), turbidity (89.47 %), TDS (94.16 %) and color (95.29 %) was observed at pH 7.12 and 0.20 g/L dosage of $CuSO_4$+$FeCl_3$ coagulant. The final pH of the solution at optimum condition for all three coagulants was under the disposal limits. Further, the flocs formed are characterized using XPS, SEM, and EDX analyses to reveal the formation of TBCC as an intermediate during the process.

4.1 Introduction

For the disposal of PRE, the government of India [133] and the World Bank Group [134] has defined the limits of the parameters pH, COD, turbidity, TDS, and color for effluent [135]. Consequently, the appropriate treatment of PRE is required for its reuse and disposal [17].

In the case of PRE, specific contaminants are heavy metals, high molecular weight aromatic hydrocarbons. The various kind of treatment processes available for PRE as discussed in chapter 1 and the prevailing literature as reported in Table 2.2 in chapter 2, inorganic metal salts like ferric chloride, ferrous sulphate, copper sulphate, poly aluminium chloride, etc. have been used as coagulants for the treatment of PRE by coagulation and flocculation process [26, 111]. The coagulation and flocculation are cost-effective, straightforward pre-treatment processes which can be extensively used on large scale for the reduction in COD, turbidity, TDS, and color of PRE by using cheap metallic salts as coagulants [49, 88, 136]. When metal salts dissolve in water, metal ion hydrates, and hydrolyzed species. These species entrap the colloidal particles by three different mechanisms: charge neutralization, adsorption, and sweep flocculation [17, 88, 89]. Hossam et al. [137] reported that the coagulation process can lower the turbidity to 1.8 NTU by ferric chloride compared to aluminium sulphate, lime, and ferrous sulphate at optimal initial pH of 8.6. Berrin et al. [138] experimentally showed centrifugation with coagulation significantly improved the petroleum hydrocarbon removal by 10-14 % and turbidity 10-35 %, respectively, by using Cat floc K-10 and Cat floc T-2. Copper salts are reported as better coagulants than iron and aluminium salts. Abolhassani et al. [139] reported copper sulphate showed a better performance in reducing microbial and organic contaminants present in municipal waste latex. Copper-based coagulant in alkaline range forms tribasic copper chloride (TBCC) which also acts as a decolorizing agent. To the best of our knowledge no work has been reported on the use of $CuSO_4$+$FeCl_3$ (cupric sulphate and ferric chloride mixed in 1:1 ratio by volume (V: V)) coagulant in comparison to cupric sulphate and ferric chloride coagulants individually, for wastewater collected from the ETP of petroleum refinery. In addition, dependent variables like final pH, COD, turbidity, TDS, and color are optimized in the selected range of variation in independent variable like pH and dosage of coagulant by response surface methodology and analysis of variance.

The efficient execution of the coagulation and flocculation treatment method depends upon the selection of appropriate independent variables for an optimum result. The conventional method of optimization where one independent variable is varied at a time keeping the other variable constant is time-consuming since multiple numbers of experiments have to perform to get the optimum condition. Also, the interaction effect of independent variables and collaborated analysis between an enormous no of independent and dependent variables becoming difficult for accurate optimization [140]. Response surface methodology (RSM) is an efficient way for the optimization of independent variables and their responses collectively and is used in different processes to achieve the highest efficiency. The RSM reduces the number of experiments significantly and has the ability to study a large number of parameters as well as the interaction between them [61]. Analysis of variance (ANOVA) provides the statistical results and diagnostic checking test, which researchers use to evaluate the adequacy of the models [141].

In this chapter, the potential and the effective pre-treatment of PRE were investigated by coagulation and flocculation process using cupric sulphate, ferric chloride, and the mixture of cupric sulphate and ferric chloride in the ration of 1:1 by volume. The experiment stratagem of RSM design with a central composite design (CCD) technique was used for optimization and effectively built models for the process independent variables in terms of their effect on dependent variables. The percentage reduction in COD, turbidity, TDS, color, and pH was observed before and after the experiments. The two factors (pH, dosage) and the five responses (final pH, COD, turbidity, TDS, and color) were used for the statistical design for optimum conditions. In addition, the nature of flocs formed is analyzed by XPS, SEM, and EDX analysis.

4.2 Materials and Methods

4.2.1 Collection of wastewater sample

PRE was collected from the flow equalization tank of the ETP from a petroleum refinery situated in October situated in Northern India. The collected wastewater was mixed with concentrated H_2SO_4 (2 ml/L) and stored in a refrigerator at 4°C to preclude the photo-catalyzed change in the PRE composition. The wastewater characteristics as listed in Table 4.1 proposed by the World Bank [135] and the Environment (protection) Rules 1986 in Schedule 1 [142] for the oil refinery industry were determined for the collected PRE samples by the standard methods immediately after the collection of wastewater [143]. The stored wastewater sample was used as such in further experiments without any dilution.

4.2.2 Chemicals

All the chemicals used during the experiments as discussed in chapter 3.

4.2.3 Analysis of wastewater

The COD and turbidity of the wastewater were determined by the standard method as discussed in chapter 3. The pH and total dissolved solids (TDS) measurements were carried out by the multi-meter real-time data logger system (ITS-601, ISO-TECH, India). The color was analyzed by the colorimeter (HI 93727, Hanna Instruments, Europe). The pH, turbidity, TDS, and color of the sample were measured after filtration through filter paper (Whatman filter paper grade-1 of pore size 11 μm). In general, there is no relationship between the turbidity and the total suspended particles in untreated wastewater. The turbidity, TDS, and color measured after filtration (after removal of all the suspended particles) increase the efficiency and preciseness of the observed data for calculations.

Table 4. 1 Characteristic of PRE and discharge standards for wastewater form petroleum refining facilities.

Parameter	**PRE (mg/L) ****	**WBG* guideline (mg/L)** [135]**	**Indian government guideline (mg/L) ** [142]**
pH	9.2	6-9	6.0-8.5
Oil &Grease (mg/l)	0.29	10	5.0
COD (mg/l)	8100	125	125
BOD	4047 (3 day, 27 °C)	30	15
TSS	19.5	30	20.0
TDS	4761	-	-
Turbidity	98	-	-
Color	550	-	-
Density	1.126	-	-
Viscosity	0.90	-	-
P	10	2	3.0
Cr(total)	3.02	0.5	2.0
Zn	0	-	5.0
Ni	4.48	0.5	1.0
Cu	2.472	0.5	1.0
V	2.80	1	0.2
Pb	2.50	0.1	0.1

As	-	0.1	-
Fe	15.54	3	-
Hg	0	0.003	0.01
Mg	83.32	-	-
Chlorides	57.14		
Phenol	238.09	0.2	0.35
Sulphate	238.09	-	-
Sulfides	3809	0.2	0.5
NaOH	0.04-0.23	-	-

*Assumes an integrated petroleum refining facility; ** All parameters in mg/l except pH in a standard unit, Turbidity in N.T.U., color in P.C.U, temperature increases in ℃, density in g/L, and viscosity in mPa.S.

4.2.4 Calculation of G value

G value is the root mean square velocity gradient, which is defined by Camp & Stein for flocculation [144] as follows:

$$G=\sqrt{\frac{W}{\mu}}$$

where W = dissipation function ($N/m^2.s$) = dissipated power per unit volume =P/V

V = volume of flocculation tank (m^3)

μ = Absolute viscosity

A good, precise protocol for centrifugation is to use the G value rather than RPM because the rotor size might differ and the g value will differ, while, the RPM stays the same. The role of power number is beneficial for a specific impeller and tank geometry, the scale-up of the pilot systems is conceivable with the same power number if the geometrical similarity is maintained. G is not the universal constant; mainly depends upon the type of chamber, kind of fluid flow, and devices. For rotating blades axial flow type of flocculation devices power consumed is given by leentwar & Ywema [144, 145] as follows:

$P = \varphi \, . \, \rho . \, n^3 \, .D^5$ N.m/s

where P= power consumed by a device

φ = dimensionless power number

ρ = liquid density (kg/m^3)

n= mixer rotational speed (revolution per second)

D= diameter of mixer impeller (m)

Therefore, G is related to the power number by [144]:

$$G=\sqrt{\frac{\varphi \, .\rho \, .n^3 D^5}{V \, . \, \mu}} \quad s^{-1}$$

The ratio of G values at different RPMs such as 200 and 30 is calculated, named G_r:

$G_r = G1/G_2$

Where, G_1 = G value at 200 RPM; G_2 = G value at 30 RPM

4.2.5 Analysis of flocs formed after coagulation and flocculation

The elemental composition and chemical state of the flocs formed during the coagulation and flocculation process in terms of their binding energy were determined using X-ray photoelectron spectroscopy (XPS, model- K-Alpha, Thermo scientific, India). The SEM and EDX were used to examine the surface morphology and to detect the elements present on the surface of flocs formed during the coagulation and flocculation as discussed in chapter 3.

4.2.6 Experimental design and data analysis

The RSM with the CCD technique was applied to optimize the process parameters. The pH (coded as A) and coagulant dosage (coded as B) were selected as independent variables, while, final pH (variation), COD, turbidity, TDS, and color reduction were selected as dependent variables. For statistical data analysis, the Design Expert Software (version 11) was used. The range of independent variables for three coagulants (cupric sulphate, ferric chloride, and 1:1 ratio (V: V), mixture of cupric sulphate and ferric chloride ($CuSO_4$+$FeCl_3$)) were selected based on preliminary experiments performed for COD reduction by each coagulant. These preliminary experiments were performed at pH ranging from 3-13 and dosage ranging from 0.15-0.95 g/L keeping the rest of the parameters such as RPM and time as constant and the respective data are given in Table 4.2, 4.3, and 4.4. Based on COD reduction the range of independent variables (pH and coagulant dosage) for all three types of coagulants was selected as mentioned in Table 4.5.

The CCD full factorial design gives thirteen experiments for each coagulant according to the eq. 1 [146], covering four factorial points (2^n), four axial points (2n), and five replicated center points (n_c). The central point varied between 3 to 10, which helped in predicting the experimental error and data reproducibility.

$$N = 2^n + 2n + n_c = 4+4+5 = 13 \tag{1}$$

where N is the total number of experimental runs that have to be performed and n is the number of independent variables.

Table 4. 2 Preliminary experimental data of coagulation and flocculation process for $CuSO_4$ coagulant.

Step 1 (constant dosage)						
pH	Dosage (g/L)	pH final	COD reduction %	Turbidity reduction %	TDS reduction %	Color reduction %
3	1	2.97	28	88	84	90
5	1	4.65	52	94	92	92
7	1	5.16	28	74	93	92
9	1	5.3	51	68	92	93.5
11	1	7.8	62	38	93	94
Step 2 (constant pH)						
pH	Dosage (g/L)	pH final	COD reduction %	Turbidity reduction %	TDS reduction %	Color reduction %
11	0.2	9.18	29	92	90.7	92
11	0.6	8.69	55	97.8	92.2	94
11	1	8.0	62	98	92.6	94
11	1.2	7.8	46	97.5	89.8	94
11	1.4	7.89	38	97	88.3	92

Table 4. 3 Preliminary experimental data of the coagulation and flocculation process for $FeCl_3$ coagulant.

Step 1 (constant dosage)						
pH	Dosage (g/L)	pH final	COD reduction %	Turbidity reduction %	TDS reduction %	Color reduction %
3	1	2.01	30	52	57	92
5	1	2.12	43	86.5	48	86
7	1	2.33	40	82	55	91
9	1	2.38	8.89	80	65	90
11	1	2.95	2.7	78	83	89
Step 2 (constant pH)						
pH	Dosage (g/L)	pH final	COD reduction %	Turbidity reduction %	TDS reduction %	Color reduction %
7	0.2	3.77	52	80	95.6	92
7	0.6	3	48	77	76	91.2
7	1	2.33	39.9	82	55	91
7	1.2	2.35	19	79	26	90
7	1.4	2.2	2	83	26	89.5

Table 4. 4 Preliminary experimental data of the coagulation and flocculation process for $CuSO_4$+ $FeCl_3$ coagulant.

Step 1 (constant dosage)						
pH	Dosage (g/L)	pH final	COD reduction %	Turbidity reduction %	TDS reduction %	Color reduction %
3	1	2.7	54	16	80	88
5	1	2.37	65	93.22	81.5	94.5
7	1	3.12	72.05	94	82.4	96.22
9	1	5.1	42	70	88.2	94.66
11	1	6.86	33	50	95	93
Step 2 (constant pH)						
pH	Dosage (g/L)	pH final	COD reduction %	Turbidity reduction %	TDS reduction %	Color reduction %
7	0.2	5	81	93	95	95.2
7	0.6	3.95	75	90	89	95.02
7	1	3.12	72.05	94	82.4	96.22
7	1.2	2.57	46	95	72	96.22
7	1.4	2.5	8	95.5	64	96.

Table 4. 5 Range of independent variable selected for CCD method.

Coagulant	pH range (S.U.)	Dosage range (g/L)
$CuSO_4$	7-11	0.6-1.2
$FeCl_3$	3-7	0.2-1.0
$CuSO_4$+$FeCl_3$	5-9	0.2-1.0

Once the range of the independent variable for each coagulant was incorporated with design expert software, the set of different experimental conditions was obtained which is provided as the experimental design matrix (Table 4.6). The experiments were performed at these set of conditions and incorporated in design expert software as actual dependent variables. Three levels were set for both pH (A) and dosage (B), such as -1 (minimum), 0 (central), +1 (maximum) for each coagulant.

After performing the experiment, the general correlation between the independent variables (pH, dosage) and response variables (final pH, COD, turbidity, TDS, and color) was acquired as:

$$Y = f(X_1, X_2, X_3, \ldots, X_n) \qquad (2)$$

where Y represents the response of the dependent variable, f is the function relates response to independent variables, and X_1, X_2, X_3,…, X_n is the n independent variables that affect the response.

The quadratic (second-order polynomial) equation was then suggested by the ANOVA technique, which was used for establishing the relation between independent and dependent variables and is expressed as:

$$Y = \beta_0 + \sum_{i=0}^{n} \beta_i x_i + \sum_{i=1}^{n} \beta_{ii} x_i^2 + \sum_{i=1}^{n-1} \sum_{j=i+1}^{n} \beta_{ij} x_i x_j + \ldots + e \qquad (3)$$

where, Y, β_0, β_i, β_{ii}, β_{ij} are the predicted response, the constant regression coefficient, the linear coefficient, the quadratic coefficient, and the interaction coefficient, respectively, and x_i, x_j are coded values of the independent variables.

The regression analysis and ANOVA were applied to study the statistical fitness of the developed model at 95% confidence level using Design-Expert software. The experimental data sets were evaluated with several variables like p-value, F-value, degree of freedom (DF), determination coefficient (R^2), adjusted determination of coefficient (R^2_{adj}), adequate precision (AP), standard deviation (SD), and coefficient of variance (CV) to check the statistical fitness of the model. F-value describes the variation in responses, which can be verified by the regression equation whereas, p-value ascertains the statistical fitness of the developed model. For a model to be significant, the p-value should be less than 0.05, and the p-value for lack of fit test should be greater than 0.05 [61]. The R^2 coefficient determines the proportion of total variation in response which indicates the ratio of sum of squares due to regression (SSR) to the total sum of square

(SST); R^2 varies from zero to one. For the satisfactory and desirable quadratic model equation of the experimental data R^2 coefficient is preferred closed to 1 [91]. Adequate precision (AP) greater than 4 indicates adequate model perception. AP is used for comparing the range of the predicted values at design point to average predicted error [140, 147]. The predicted vs. actual values plot and three dimensional (3D) RSM plot were used to investigate the optimum condition of responses stimulated by the varied independent variables. A CV indicates experimental reliability and precision [148].

4.2.7 Experimental setup and the process

The coagulation and flocculation process was executed by jar test apparatus (IK-155, IKON, India) with an inserted rectangular paddle blade (2 paddle blade of dimensions 0.05 m x 0.02 m x 0.0072 m) in the impeller. A jar test is aimed to remove the non-settable, suspended, and colloidal matter from the effluent, which leads to the reduction of COD, turbidity, TDS, and color. The experiments were performed at the set of conditions provided by the design expert software as mentioned in Table 4.6 considering pH and dosage as independent variables. The rest of the parameters such as rapid and slow mixing RPM (revolutions per minute) and settling time were selected from the literature [24, 88, 136]. Accordingly, the coagulation (during jar test operation) was performed for 5 min at 200 RPM using rapid mixing, and flocculation was performed for 20 min at a slow mixing speed of 30 RPM followed by the 45 min settling time. A similar procedure was followed for all three coagulants separately. The final supernatant obtained after centrifugation has subjected to COD analysis. The supernatant after the filtration by the Whatman filter paper of pore size- 11 µm was used for the analysis of pH, turbidity, TDS, and color. All the experiments were performed twice and the average value has been reported.

4.3 Result and discussion

4.3.1 Statistical analysis

The response surface methodology (RSM) is used for the procurement of collaborative optimum result for two independent variables (pH and dosage) and five dependent variables (final pH, COD, turbidity, TDS, and color reduction) analyses of the effect of $CuSO_4$, $FeCl_3$ and $CuSO_4$+$FeCl_3$ coagulants by coagulation-flocculation for PRE. The CCD legitimated the development of mathematical equation shown in Table 4.7, where predicted response (Y) were assessed as a function of pH (A) and coagulant dosage (B) and was calculated as the sum of a constant, two first-order coefficient (in terms of A and B), one interaction effect (AB), and two-second order effects (A^2, and B^2) according to equation 3. The mathematical equations obtained from ANOVA were used to analyze the "goodness of fit".

4.3.2 Effect of coagulants on final pH

The relation between the predicted and experimental values of final pH for $CuSO_4$, $FeCl_3$, and $CuSO_4$+$FeCl_3$ coagulants is shown in Fig. 4.1 (a), 4.2 (a), and 4.3 (a) respectively. The graphs clearly show that both actual and predicted values of the response are in close agreement, which interprets that the model developed for final pH is well-matched to form a relationship among independent and dependent variables during coagulation and flocculation processes. The value of correlation coefficient (R^2) for a response (final pH) in the case of $CuSO_4$, $FeCl_3$, and $CuSO_4$+$FeCl_3$ coagulants was found to be 0.9972, 0.9800, and 0.9937, respectively, and showed a reliable relation between dependent and independent variables. This also elucidated that the total variation explained by the developed model was 99.72, 98, and 99.37 %, and there might be 0.28, 2, and 0.63 % of the total variation that cannot be explained by the developed model. The R^2_{adj} for a response (final pH) for $CuSO_4$, $FeCl_3$, and $CuSO_4$+$FeCl_3$ coagulants was found to be

Table 4. 6 Set of experimental conditions of independent variables (pH and dosage) and response (final pH, COD, turbidity, TDS, and color) for $CuSO_4$, $FeCl_3$, and $CuSO_4$+$FeCl_3$coagulants.

Run. No.	$CuSO_4$							$FeCl_3$							$CuSO_4$+ $FeCl_3$						
	Independent variables		Responses					Independent variables		Responses					Independent variables		Responses				
	A: Initial pH (S.U.)	B: Dosage (g/L)	Final pH(S.U.)	COD reduction (%)	Turbidity reduction (%)	TDS reduction (%)	Color reduction (%)	A: Initial pH (S.U.)	B: Dosage (g/L)	Final pH (S.U.)	COD reduction (%)	Turbidity reduction (%)	TDS reduction (%)	Color reduction (%)	A: Initial pH (S.U.)	B: Dosage (g/L)	Final pH(S.U.)	COD reduction (%)	Turbidity reduction (%)	TDS reduction (%)	Color reduction (%)
1	***11***	***0.6***	***8.69***	***55***	***97.8***	***92.2***	***94***	5	0.6	2.33	49	86.2	54	87	7	0.6	3.8	75.5	91.5	88.1	95.08
2	7	0.6	5.5	39.5	87	94	92	7	0.6	3	48	77	76	91.2	5	0.2	3.41	71	92	90.5	94.5
3	7	0.9	5.29	41.8	79.5	93	92.5	5	0.6	2.2	48.8	85	55	87.7	7	0.6	3.81	74.5	89	89.5	94.92
4	11	0.9	8.13	55.6	98	91.6	94.5	5	0.6	2.29	50.2	84	56	87.2	5	1	2..37	65	93.22	81.5	94.5
5	9	0.6	6.1	48	70	91.5	93	5	0.6	2.31	50.7	86	53	86.9	7	1	3.12	72	94	82.4	96.22
6	7	1.2	5	41.5	88.5	90	93	***7***	***0.2***	***3.7***	***52***	***80***	***95.5***	***92***	5	0.6	2.5	69.72	93	86	93.75
7	9	0.9	5.61	51	69	92	93	3	0.2	2.3	34	49	62	93	***7***	***0.2***	***5***	***81***	***93***	***95***	***95.2***
8	9	1.2	5.1	45	68.5	88.5	93.5	5	0.2	2.9	58.5	85	60	89	9	0.2	6.9	40	61	97.8	93.4
9	9	0.9	5.6	50	67	91.5	93.2	5	1	2.12	43	86.5	48	86	9	0.6	5.8	41	65	93	93.22
10	9	0.9	5.55	50.5	68	91.75	93.1	7	1	2.33	40	82	55	91	9	1	5.1	42	70	88.2	94.66
11	9	0.9	5.62	48.8	66	91.25	93.2	3	1	2	30	52	57	92	7	0.6	4	76.5	91	88	94.9
12	11	1.2	7.8	46	97.5	89.8	94	3	0.6	2.2	32	50	60	92.5	7	0.6	3.9	73	89	89.5	94.82
13	9	0.9	5.69	52.1	70	91.5	92.7	5	0.6	2.32	48	83	57	87.2	7	0.6	3.95	75	90	89	95.02

Table 4. 7 ANOVA results of the response variable for $CuSO_4$, $FeCl_3$ and $CuSO_4$+$FeCl_3$ coagulants

Responses	**Final equation in terms of code of independent variables**	**P**	**F**	**R^2**	**R^2_{adj}**	**AP**	**SD**	**CV %**	**DF**
$CuSO_4$									
Final pH	$5.61 + 1.47\,A - 0.3983\,B - 0.0975\,AB + 1.21\,A^2 + 0.0109\,B^2$	< 0.0001	496.49	0.9972	0.9952	64.5175	0.0853	1.39	5
COD	$50.37 + 5.63\,A - 1.67\,B - 2.75\,AB - 1.40\,A^2 - 3.60\,B^2$	< 0.0001	37.05	0.9636	0.9376	19.4554	1.27	2.64	5
Turbidity	$67.63 + 6.38\,A - 0.0500\,B - 0.4500\,AB + 22.05\,A^2 + 2.55\,B^2$	< 0.0001	67.24	0.9796	0.9650	19.1175	2.42	3.07	5
TDS	$91.49 - 0.5667\,A - 1.57\,B + 0.4000AB + 1.09\,A^2 - 1.21\,B^2$	< 0.0001	38.01	0.9645	0.9391	22.1289	0.3450	0.37	5
Color	$93.09 + 0.9167\,A + 0.3333\,B - 0.1250\,AB + 0.2983\,A^2 + 0.0483\,B^2$	0.0001	29.35	0.9545	0.9219	18.0464	0.2039	0.21	5
$FeCl_3$									
Final pH	$2.32 + 0.4217\,A - 0.4083\,B - 0.2675\,AB + 0.1953\,A^2 + 0.1053\,B^2$	< 0.0001	68.59	0.9800	0.9657	28.9648	0.0865	3.51	5
COD	$49.71 + 7.33\,A - 5.25\,B - 2.00AB - 10.52\,A^2 + 0.2269\,B^2$	< 0.0001	41.49	0.9674	0.9440	19.0979	2.03	4.52	5
Turbidity	$84.66 + 14.67\,A + 1.08B - 0.2500\,AB - 20.69\,A^2 + 1.56\,B^2$	< 0.0001	281.78	0.9951	0.9915	41.0969	1.36	1.80	5
TDS	$54.95 + 7.92\,A - 9.58\,B - 8.87\,AB + 13.18\,A^2 - 0.8190\,B^2$	< 0.0001	51.21	0.9734	0.9544	27.4400	2.64	4.35	5
Color	$87.24 - 0.5467\,A - 0.8333\,B + 0.0000\,AB + 4.57\,A^2 + 0.2125\,B^2$	< 0.0001	59.27	0.9769	0.9604	19.7182	0.5066	0.56	5
$FeCl_3$ + $CuSO_4$									
Final pH	$3.87 + 1.59\,A - 0.7867\,B - 0.1900\,AB + 0.3193\,A^2 + 0.2293\,B^2$	< 0.0001	221.82	0.9937	0.9892	52.5019	0.1331	3.22	5
COD	$75.24 - 13.79\,A - 2.17\,B + 2.00\,AB - 20.73\,A^2 + 0.4124\,B^2$	< 0.0001	126.73	0.9891	0.9813	27.2064	2.01	3.05	5
Turbidity	$90.56 - 13.70\,A + 1.87\,B + 1.95\,AB - 12.71\,A^2 + 1.79\,B^2$	< 0.0001	122.02	0.9887	0.9806	28.8259	1.64	1.92	5
TDS	$88.80 + 3.50\,A - 5.20\,B - 0.1500\,AB + 0.7379\,A^2 - 0.0621\,B^2$	< 0.0001	57.44	0.9762	0.9592	28.1665	0.9093	1.02	5
Color	$94.95 - 0.2450\,A + 0.3800\,B + 0.3150\,AB - 1.45\,A^2 + 0.7707\,B^2$	< 0.0001	113.19	0.9878	0.9791	36.1623	0.1160	0.12	5

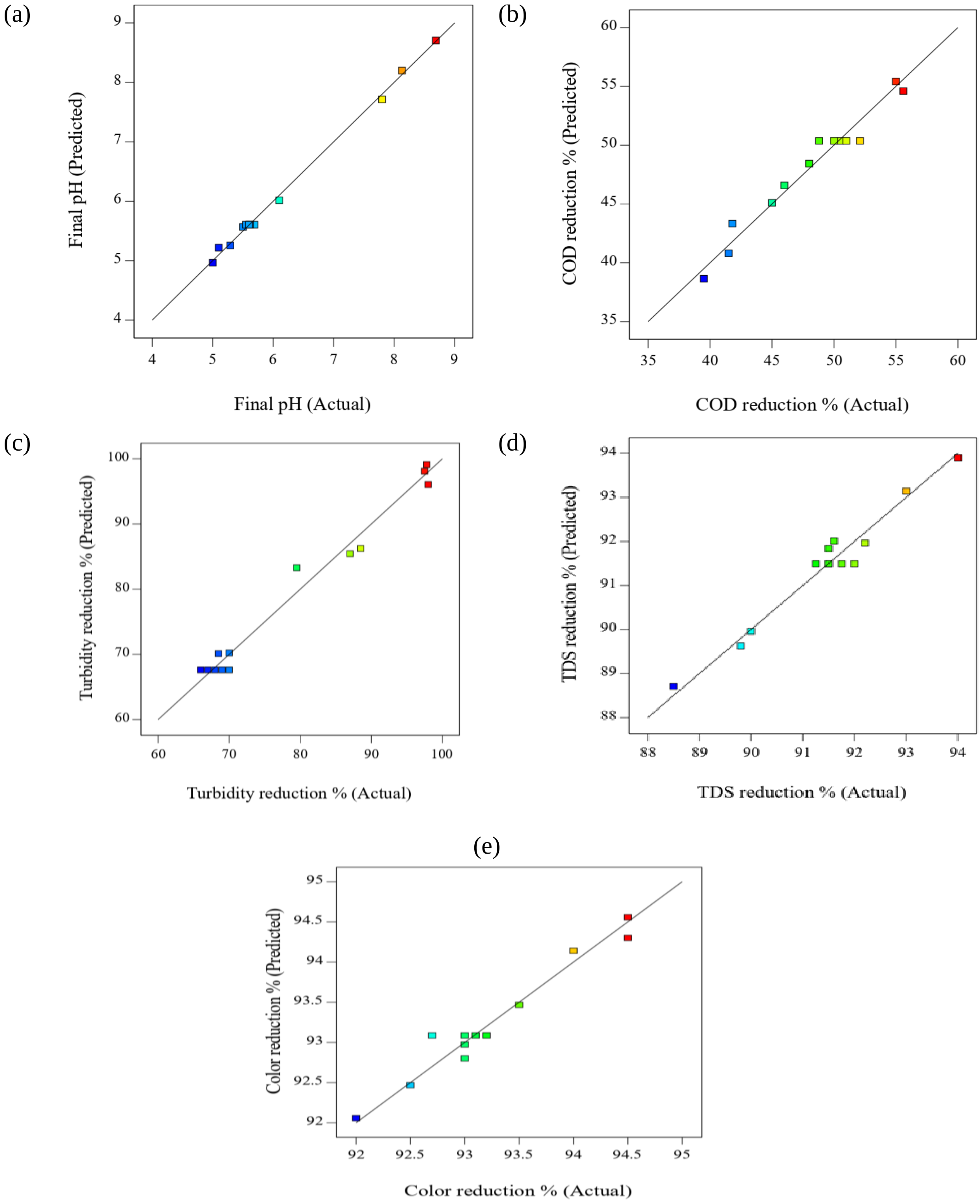

Figure 4. 1 Design expert plot, predicted vs. actual plot for $CuSO_4$ coagulant (a) Final pH (b) COD reduction (c) turbidity reduction (d) TDS reduction (e) color reduction.

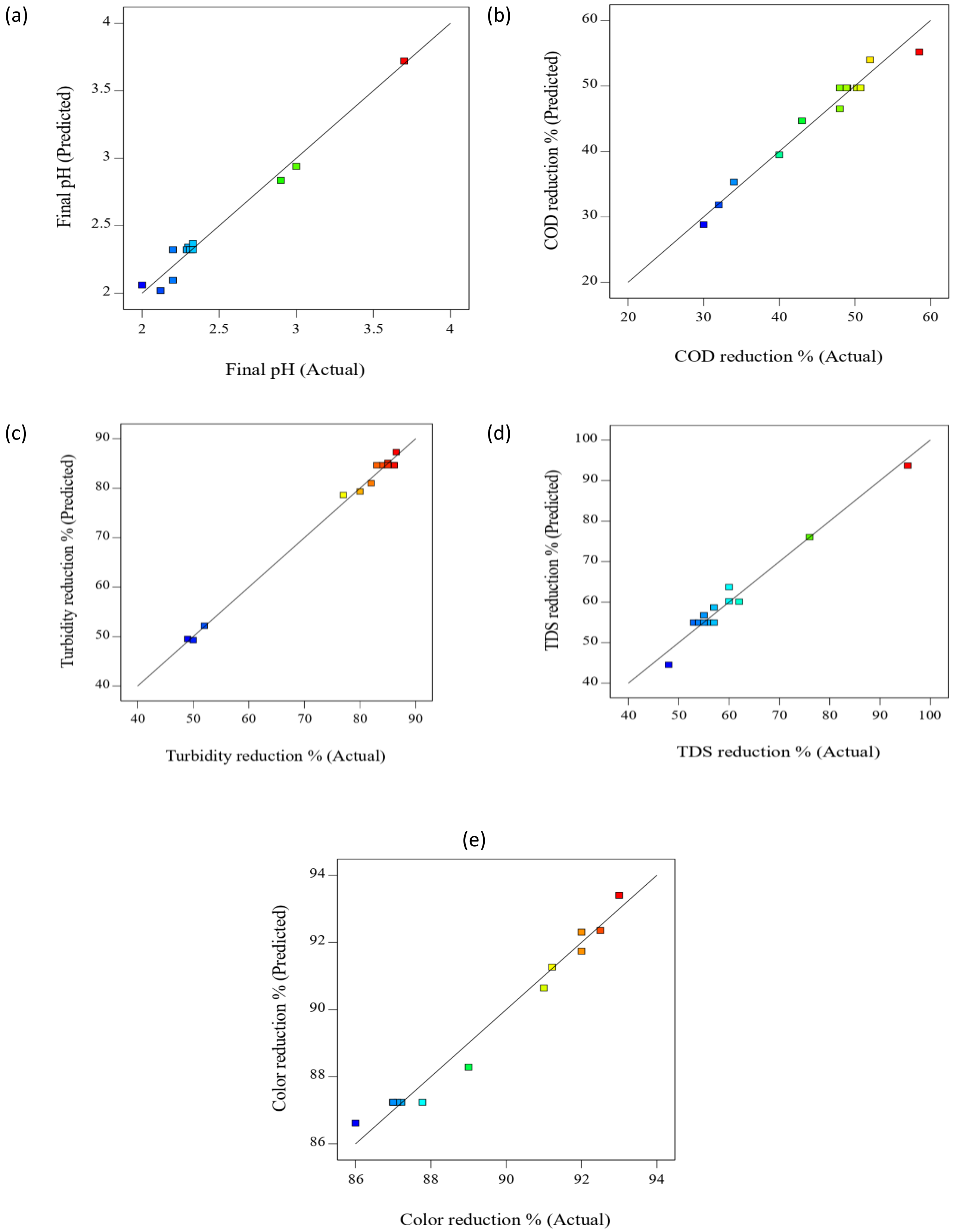

Figure 4. 2 Design expert plot, predicted vs. actual plot for $FeCl_3$ coagulant (a) Final pH (b) COD reduction (c) turbidity reduction (d) TDS reduction (e) color reduction.

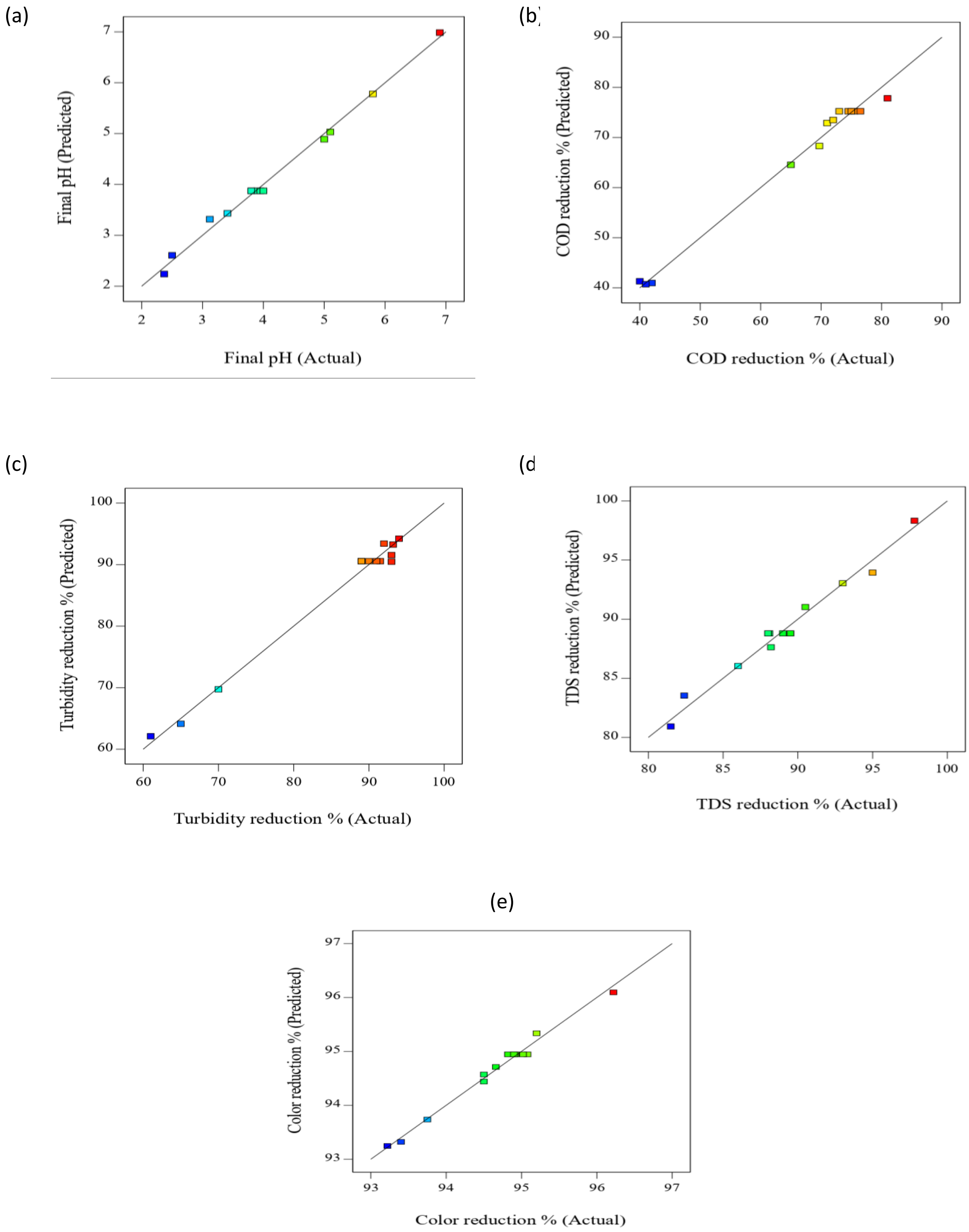

Figure 4. 3 Design expert plot, predicted vs. actual plot for $CuSO_4$+$FeCl_3$ coagulant (a) Final pH (b) COD reduction (c) turbidity reduction (d) TDS reduction (e) color reduction.

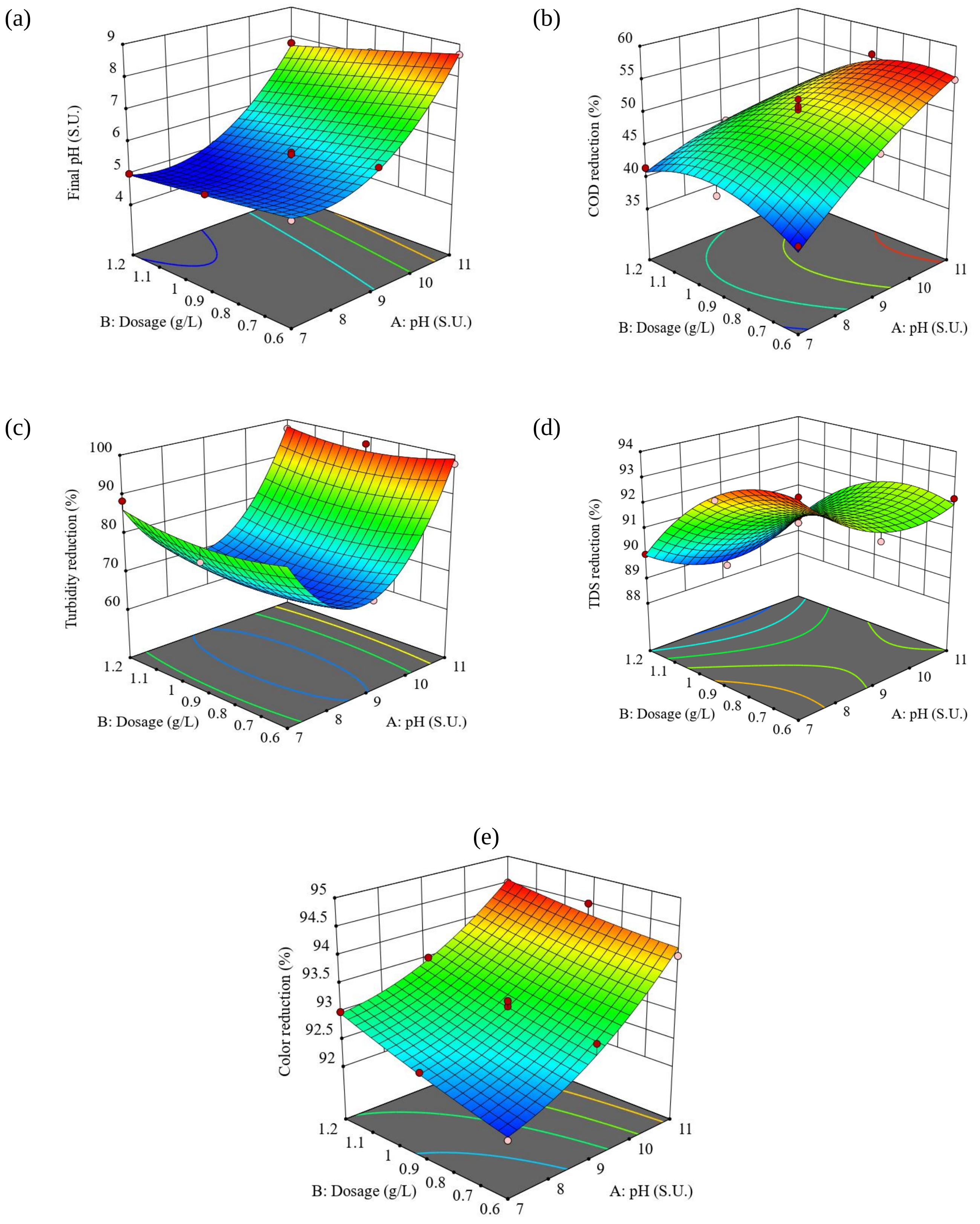

Figure 4. 4 Design expert plot; response surface 3D plot for $CuSO_4$ coagulant (a) Final pH (b) COD reduction (c) turbidity reduction (d) TDS reduction (e) color reduction.

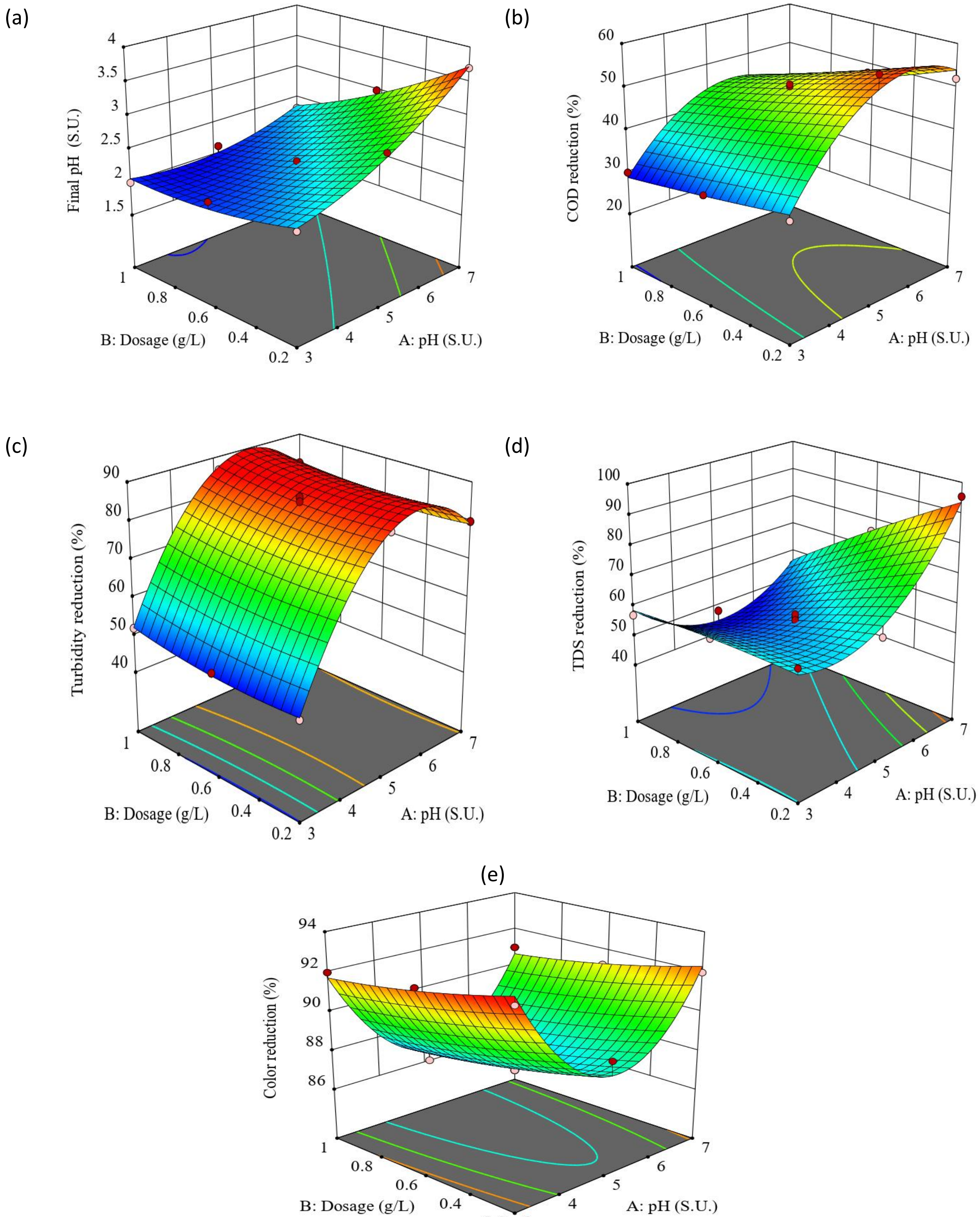

Figure 4. 5 Design expert plot; response surface 3D plot for $FeCl_3$ coagulant (a) Final pH (b) COD reduction (c) turbidity reduction (d) TDS reduction (e) color reduction.

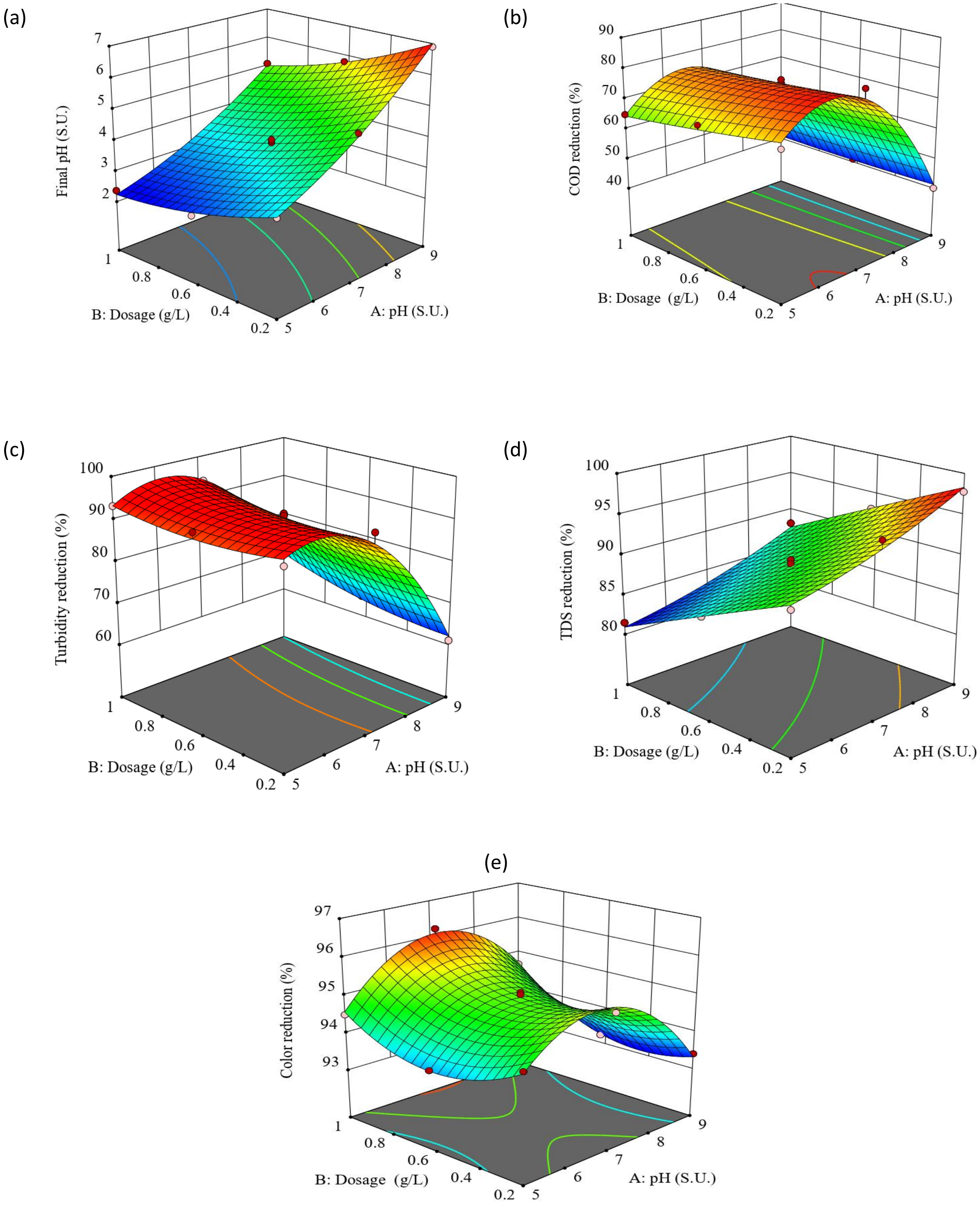

Figure 4. 6 Design expert plot; response surface 3D plot for $CuSO_4$+$FeCl_3$ coagulant (a) Final pH (b) COD reduction (c) turbidity reduction (d) TDS reduction (e) color reduction.

0.9952, 0.9657, and 0.9892, which were very close to R^2 value as shown in Table 4.7. Thus, the prediction of experimental data is deliberately satisfactory. The relationships developed through ANOVA between independent variables (pH (A), dosage (B)), and dependent variables (final pH, COD, TDS, turbidity, and color reduction) for $CuSO_4$, $FeCl_3$, and $CuSO_4$+$FeCl_3$ coagulants are presented in Table 4.7 in the form of quadratic equations. The positive terms of the equations indicate a favorable effect, whereas the negative sign indicates the antagonistic effect of each factor. For final pH, in the case of $CuSO_4$, $FeCl_3$, and $CuSO_4$+$FeCl_3$ coagulants, parameters B had a more negative effect as compared to AB for all three coagulants. While other parameters such as A, A^2, and B^2 had a positive effect on the response.

The significance of an independent variable was also evaluated in terms of p and F-values. For response (final pH), in the case of $CuSO_4$, $FeCl_3$, and $CuSO_4$+$FeCl_3$ coagulants, the p-value was less than 0.0001 in each case, while F-value was found to be 496.49, 68.59, and 221.82 respectively. The AP for a response (final pH) was found to be 64.517, 28.9648, and 52.5019 for $CuSO_4$, $FeCl_3$, and $CuSO_4$+$FeCl_3$ coagulants, respectively. This inferred that the developed response equation can be used within a range defined for designing. The model reproducibility is interpreted in terms of coefficient of variance (CV) and the model is considered as reproducible when a CV is less than 10%. For response (final pH), in the case of $CuSO_4$, $FeCl_3$, and $CuSO_4$+$FeCl_3$ coagulants, the CV was 1.39, 3.51, and 3.224 %, respectively, justifying very good precision and reliability of the developed model.

The three-dimensional (3D) plots of the dependent variable (final pH) at the optimum condition were obtained to verify the dependence of independent variable (pH and dosage) for $CuSO_4$, $FeCl_3$, and $CuSO_4$+$FeCl_3$ coagulants. The results are shown in Fig. 4.4 (a), 4.5 (a), and 4.6 (a), respectively. The response (final pH) for $CuSO_4$, $FeCl_3$, and $CuSO_4$+$FeCl_3$ coagulants increased with the increases in pH of PRE and decreased with the increase in dosage. The maximum final pH was attained at high pH and low dosage, whereas the lowest final pH was found at low pH and high dosage. In the case of $CuSO_4$, the value of final pH was higher than $FeCl_3$, and $CuSO_4$+$FeCl_3$. The range of final pH for $FeCl_3$, with an increase in pH and dosage, was very small as shown in Fig. 4.5(a); this might be due to the higher acidic nature of ferric chloride solution in water. In case of $CuSO_4$+$FeCl_3$, the final pH was found in between the $CuSO_4$ and $FeCl_3$. Also, final pH in the case of $CuSO_4$ and $CuSO_4$+$FeCl_3$ as coagulant was found in the safe zone for disposal of PRE after treatment. Experimentally, it was observed that the pH of 1.0 g/L concentration solution for $CuSO_4$, $FeCl_3$, and $CuSO_4$+$FeCl_3$ coagulants was 4.16, 1.70, and 2.01, respectively. This showed that the mixing of coagulants can change the pH of the solution during coagulation process. The pH value refers to the number of hydrogen ions present in a medium [149]. As described by the precipitation theory of the ions i.e. metal salt when mixed with water, release the metal cations and hydronium ion which consequently makes any medium too acidic [150]. The $CuSO_4$ in water forms Cu^{+2} and SO_4^{-2} ions, which are hydrolyzed to $CuOH^{(+)}$, Cu $(OH)_2$, and $H_3O^{(+)}$. The release of the hydronium (hydrogen) ions by hydrolysis is responsible for the acidic nature of the aqueous solution of $CuSO_4$. $FeCl_3$ in water forms $Fe(OH)_2^{-}$, $Fe(OH)^{-2}$, $Fe(OH)_3$, $H_3O^{(+)}$ and HCl; where the formation of HCl and $H_3O^{(+)}$ ions makes it highly acidic. The mixture $CuSO_4$+$FeCl_3$ contains both the HCl, $H_3O^{(+)}$ and SO_4^{-2} ions, which make it more acidic than $CuSO_4$and less acidic than the $FeCl_3$ [130]. According to the 3D graph projection of $CuSO_4$+$FeCl_3$ coagulant in Fig. 4.6 (a), and considering the optimum collaborated value of all dependent variables for all three types of coagulants, the $CuSO_4$+$FeCl_3$ coagulant best among the all at high pH and low dosage in the range selected independent parameters. The $FeCl_3$ coagulant is not suggested as the coagulant for the treatment of PRE due to the highly acidic nature of the coagulant solution. As per the government rules of disposal of wastewater in water bodies, the pH of wastewater must be lies between 5 to 9. The range of final pH for $FeCl_3$, at all the combination of pH and dosage, selected for coagulation process was less than 3.7. Therefore, it is considered as an acid salt, and the wastewater must hold adequate alkalinity (natural or added) to react with the acid as it forms to sustain the pH within the preferred range for good coagulation and flocculation.

4.3.3. Effect of coagulants on COD

The relation between the actual and predicted values of COD reduction for $CuSO_4$, $FeCl_3$, and $CuSO_4$+$FeCl_3$ coagulants are shown in Fig. 4.1 (b), 4.2 (b), and 4.3 (b), respectively. It can be seen that both actual and predicted values are very close to each other, which indicates that the developed model is reliable enough to establish relationship between the dependent and independent variables. The R^2 and R^2_{adj}values for COD reduction in case of $CuSO_4$, $FeCl_3$, and $CuSO_4$+$FeCl_3$ were found to be 0.9636, 0.9674, and 0.9891, and 0.9376, 0.9440, and 0.9813, respectively, as listed in Table 4.7. The higher values of both R^2 and R^2_{adj} attribute to the excellent and reliable fitting of the developed model. The R^2_{adj}values are very close to R^2 value, which signifies that the developed model is significant. The relationship between independent and dependent variables in the form of a quadratic equation for COD reduction in the case of $CuSO_4$, $FeCl_3$, and $CuSO_4$+$FeCl_3$ coagulants are given in Table 4.7. For $CuSO_4$, the terms B, AB, A^2 and B^2 had negative effects, while, A had a positive effect on the response variable. For $FeCl_3$ coagulant, B, AB, and A^2 had negative effects, while, A and B^2 had positive effects on the response. This might be due to an increase in COD reduction with an increase in pH in the range of 7-11 and 3-7 for $CuSO_4$, and $FeCl_3$, respectively, as well as an increase in dosage in the range of 0.6-1.2 and 0.2-1.0 g/L, for $CuSO_4$ and $FeCl_3$, respectively. In the case of $CuSO_4$+$FeCl_3$ coagulant A, B, and A^2 had negative effects, however, AB and B^2 had a positive impact on the response at pH ranging from 5 to 9 and dosage ranging from 0.2 to 1.0 g/L. The statistical analysis for COD reduction as mentioned in Table 4.7, showed that for $CuSO_4$, $FeCl_3$, and $CuSO_4$+$FeCl_3$

coagulants, F-value was noted to be 37.05, 68.59, and 126.73 respectively, and the p-value was less than 0.0001 for all three coagulants. This revealed that the model developed by ANOVA is well suited to establish the relation between independent and dependent variables for all coagulants. The AP measured for COD reduction was 19.4554, 19.0979, and 27.2064 for $CuSO_4$, $FeCl_3$, and $CuSO_4$+$FeCl_3$ coagulants, respectively, and indicated that the developed response equation can be used within a range defined for designing. For COD reduction, the CV for $CuSO_4$, $FeCl_3$, and $CuSO_4$+$FeCl_3$ coagulants was found to be 2.64, 4.52, and 3.05; indicated the precision and reliability of the response model was very good. The R^2, p-value, F-value, AP, and CV for $CuSO_4$+$FeCl_3$ coagulant was found to be best among the three coagulants by ANOVA, and thus it can be attributed that the model developed for COD reduction for $CuSO_4$+$FeCl_3$ coagulant was more desirable, precise, and reliable for design purpose.

The 3D plots for COD reduction at the optimum condition were achieved to examine the effect of independent variables (pH and dosage). The results for $CuSO_4$, $FeCl_3$, and $CuSO_4$+$FeCl_3$ coagulants are shown in Fig. 4.4 (b), 4.5 (b), and 4.6 (b), respectively. For $CuSO_4$ (Fig. 4.4 (b)), the COD reduction increased with the increase in pH, while, with an increase in dosage, COD reduction increased up to a maximum value then start decreasing. The maximum COD reduction was observed at high pH and low dosage. For $FeCl_3$ (Fig. 4.5 (b)), COD reduction was increased with the increase in pH, while with the increase in dosage, the COD reduction, increased in the lower range of pH and decreased in the higher range of pH. The optimum COD reduction was obtained at low pH and high dosage. However, in the case of $FeCl_3$, the desirable range predicted by the ANOVA was at high pH and low dosage. This might be due to parallel and interactive effect of other dependent variables. Final pH of the solution at lower pH and high dosage became highly acidic, which would not be fit for disposal. In case of $CuSO_4$+$FeCl_3$ coagulant, the reduction in COD first increased with the increase in pH up to 7, after that COD reduction suddenly decreased with a dosage in the range of 0.2- 1.0 g/L. With an increase in dosage, the COD reduction decreased between the pH ranges from 5 to 7, however, after pH 9, the COD reduction increased with the increase of dosage. The maximum COD reduction was observed around 7 pH and lower dosage as shown in Fig. 4.6 (b).

The maximum COD reduction could be observed by a coagulant at a condition where the combined effect of charge neutralization, adsorption, and sweep flocculation will occur at maximum rates. When the metal salts are dissolved in water, the metal ion hydrolyzed and hydrated to form mono and polymeric species like MOH^{+2}, $M(OH)_2^{+}$, $M_2(OH)_2^{4+}$, $M(OH)_4^{5+}$, $M(OH)_3^{0}$ and $M(OH)_4^{-}$. When these cations are hydrolyzed, the chloride and sulfates ions forms are very soluble and non-reactive in solution. In the acidic range, principally charge neutralization occurs, where the negative charge ions present in PRE are neutralized with the positively charged metal species. The adsorption occurs generally in the alkaline range, where the cations of metal ions form an insoluble complex and metal hydroxide having a positive charge (have a large surface area and are amorphous and hydrophobic in nature) get attached to the negatively charged (anionic) particles present in PRE. The $CuSO_4$+$FeCl_3$ coagulant in the pH range 4-7 and $CuSO_4$ in the alkaline range (in presence of chloride ion) reacts as per the following reactions respectively [151, 152]:

$$CuSO_4 + H_2O \rightarrow Cu^{+2} + SO_4^{-2} + OH^{-} + H^{+} \quad (4)$$

$$FeCl_3 + H_2O \rightarrow Fe^{+3} + 3Cl^{-} + OH^{-} + H^{+} \quad (5)$$

$$3\,CuSO_4 + 2\,FeCl_3 \rightarrow Fe_2(SO_4)_3 + 3CuCl_2 \quad (6)$$

The NaOH present in the PRE reacts with $CuCl_2$to form $Cu_2(OH)_3Cl$ during the coagulation and flocculation process.

$2\ CuCl_2 + 3\ NaOH \rightarrow Cu_2(OH)_3Cl + 3\ NaCl$ (7)

If sufficient chloride ions are present in solution, hydrolysis of $CuSO_4$ with alkali also produces $Cu_2(OH)_3Cl$ [151].

$2\ CuSO_4 + 3\ NaOH + NaCl \rightarrow Cu_2(OH)_3Cl + 2\ Na_2SO_4$ (8)

Tribasic copper chloride, $Cu_2(OH)_3Cl$ (TBCC) used as a chemical intermediate or proceeding intermediate in industries. It is virtually insoluble in water and organic solvents, and largely soluble in neutral medium and decomposes above 220 °C [152]. TBCC is also used as a catalyst [153], a photo-catalyst, and a decolorizing agent [154]. TBCC has high density and a 3D octahedron edge linked and parallel layered structure [151, 155], which enhances the adsorption and settling characteristics in water. The maximum COD reduction from Eq. 7 and 8, for $CuSO_4$+$FeCl_3$ (at a lower dosage and pH 7) and $CuSO_4$ (with alkali) coagulant has attributed the formation of TBCC intermediate, respectively. The speciation diagram of Fe (III) [118] and Cu (II) [155] represents the variation in ion formation by coagulant in wastewater. The Fe^{+3} ion in an acidic medium below pH 5 exists in the form of Fe^{+3}, $Fe(OH)^{+2}$ and $Fe(OH)_2^{+}$. For $FeCl_3$, maximum COD reduction at pH 5.0 and dosage 0.2 g/L was due to the charge neutralization. The $CuSO_4$ at pH above 8 exists as $Cu(OH)_3^{-}$, $Cu(OH)_4^{-2}$ and $Cu(OH)_2$. The maximum COD reduction in case of $CuSO_4$ was attained at pH 11 and dosage 0.74 g/L due to adsorption, sweep flocculation, and the TBCC formation. The maximum COD removal observed for $CuSO_4$ and $CuSO_4$+$FeCl_3$ coagulant is due to the simultaneous effect of adsorption, sweep flocculation and formation of TBCC. $CuSO_4$+$FeCl_3$ coagulant was found to be most effective coagulant among the three coagulants used for coagulation and flocculation process of PRE.

4.3.4 Effect of coagulants on turbidity

The relation between actual and predicted values of response (turbidity reduction) established by ANOVA for $CuSO_4$, $FeCl_3$, and $CuSO_4$+$FeCl_3$ coagulants, is shown in Fig. 4.1 (c), 4.2 (c), and 4.3 (c), respectively. The results showed that actual and predicted values are close to each other for all three coagulants justifying that the developed model is reliable enough for predicting the response. The value of correlation coefficients R^2 and R_{adj}^2values for turbidity reduction in case of $CuSO_4$, $FeCl_3$, and $CuSO_4$+$FeCl_3$ coagulants are 0.9796, 0.9951 and 0.9887, and 0.9650, 0.9915 and 0.9806, respectively. This suggests the unfailing relation between the dependent and independent variables. The quadratic relationship established between independent (pH (A), dosage (B)), and dependent variable (turbidity reduction) for coagulants $CuSO_4$, $FeCl_3$, and $CuSO_4$+$FeCl_3$ is shown in Table 4.7. For $CuSO_4$, the parameters B and AB had a negative effect on the turbidity reduction, while, parameters A, A^2 and B^2 had a positive effect on turbidity reduction. In the case of $FeCl_3$, parameters AB and A^2 had a negative effect, and A, B, and B^2 had a positive effect on the turbidity reduction. For $CuSO_4$+$FeCl_3$ as a coagulant, A and A^2 had a negative effect, however, parameters B, AB, B^2 had a positive effect on the turbidity reduction.

The ANOVA confirmed that for turbidity reduction in the case of $CuSO_4$, $FeCl_3$, and $CuSO_4$+$FeCl_3$ coagulants, the p-value is less than 0.0001 for all coagulants, and F-value is 67.24, 281.78, and 122.02, respectively. This signifies that the model developed by ANOVA is appropriately applicable. The AP measured for response in case of $CuSO_4$, $FeCl_3$, and $CuSO_4$+$FeCl_3$ coagulants were found to be 19.117, 41.0969, and 28.8259, respectively. This indicates that the developed model can be used within a well-defined array for designing. The CV for turbidity reduction in case of $CuSO_4$, $FeCl_3$, and $CuSO_4$+$FeCl_3$ coagulants was found to be 3.07, 1.80, and 1.92, respectively, which indicated that precision and reliability of the response model was upright.

Fig. 4.4 (c), 4.5 (c) and 4.6 (c) show the 3D response surface plots for $CuSO_4$, $FeCl_3$, and $CuSO_4$+$FeCl_3$ coagulants. It was investigated to study the effect of change in the independent variable on dependent variables. Turbidity is measured in terms of scattering of light caused by both inorganic colloids and organic matter present in PRE. The electrical charge of inorganic colloids in wastewater form adsorption and desorption surface for anions, cations, and all other charged materials [156]. In addition, the turbidity of PRE might be due to colored particles dissolved in PRE. In the coagulation and flocculation process, coagulant treatment breaks the colloidal suspension of anions and cations present in PRE through the Brownian movement [88, 157]. This is attributed to a decrease in the turbidity of PRE by any or combined effect of neutralization, adsorption, and sweep flocculation. The combined effect of pH and dosage were studied for all three coagulants. For $CuSO_4$, the turbidity reduction first decreased up to a certain value with an increase in pH and dosage and then started increasing on further increase in pH and dosage. The turbidity reduction was optimum at high pH and at all defined range of dosage for $CuSO_4$. On other hand, the opposite trend with respect to $CuSO_4$ for turbidity reduction was observed in case of $FeCl_3$. With the increase in pH, the turbidity reduction initially increased, and then after a certain pH, it decreased, however, the dosage variation reflected the opposite trend. The effect of change in dosage variation for $FeCl_3$ was minimal. The maximum turbidity removal was observed above pH 5 in the defined range. For $CuSO_4$+$FeCl_3$ coagulant, the turbidity reduction decreased with an increase in pH, while it increased with an increase in dosage. From the speciation diagram, it can be observed that $CuSO_4$ above pH 9 and $FeCl_3$ above pH 5 forms the metal salt such as $M(OH)_x^0$ and $M(OH)_x^-$ ions (M: Cu^{+2} and Fe^{+3}). This salt formation attributed to maximum turbidity reduction through adsorption and sweep flocculation, leaving the charge neutralization less effective for PRE. Thus, the organic and inorganic compounds present in PRE were removed principally by adsorption and sweep flocculation. For $CuSO_4$+$FeCl_3$

coagulant, the range of pH for major turbidity reduction was from 5 to 8 which were between the other two coagulants ($CuSO_4$ and $FeCl_3$). The TBCC formed in case of $CuSO_4$ and $CuSO_4$+$FeCl_3$ as coagulants enhanced the turbidity reduction due to its tendency to form larger floc size and its decolorizing properties.

4.3.5 Effect of coagulants on TDS reduction

For TDS reduction the relation between actual and predicted values for $CuSO_4$, $FeCl_3$, and $CuSO_4$+$FeCl_3$ are presented in Fig. 4.1 (d), 4.2 (d), and 4.3 (d) respectively. The close agreement between actual and predicted values showed that the developed model is reliable enough to establish the relation between independent and dependent variables. The value of correlation coefficients R^2 and R_{adj}^2values for TDS reduction in case of $CuSO_4$, $FeCl_3$, and $CuSO_4$+$FeCl_3$ coagulants are 0.9645, 0.9734, and 0.9762, and 0.9391, 0.9544, and 0.9592, respectively. This suggests the unfailing relation between the dependent and independent variables. The quadratic relationship established between independent (pH (A), dosage (B)) and dependent variable (TDS reduction) for coagulants $CuSO_4$, $FeCl_3$, and $CuSO_4$+$FeCl_3$ is shown in Table 4.7. In case of $CuSO_{4,}$ the parameters A, B, and B^2 had a negative influence, while, AB and A^2 had a positive influence. For $FeCl_3$ and $CuSO_4$+$FeCl_{3,}$ the parameters B, AB, B^2 had a negative influence, while, A and A^2 had a positive influence. In addition, the statistical fitness of developed model for a response (TDS reduction) for all three coagulants was also examined by p-value, F value, AP, and CV. The results are presented in Table 4.7. Results show that in every aspect the developed model for TDS reduction is reliable and significant.

A total dissolved solid (TDS) is a measurement of inorganic salts, organic matter, and other dissolved materials in water [1]. The 3D plots for turbidity reduction for $CuSO_4$, $FeCl_3$, and $CuSO_4$+$FeCl_3$ coagulants are shown in Fig. 4.4 (d), 4.5 (d), and 4.6 (d), respectively, to examine the effect of pH and dosage on TDS reduction. TDS are solids which totally dissolved and form a homogenous mixture. For $CuSO_4$, TDS reduction initially decreased with an increase in pH, and after pH 9 is increased. However, with a change in dose, an opposite trend was observed for TDS reduction in a neutral and highly basic medium as shown in Fig. 4.4(d). Thus, for $CuSO_4$, the optimum TDS reduction was observed at lower pH and lower dosage. This might be attributed to charge neutralization. In case of $FeCl_3$, the TDS reduction increased with the increase in pH and decreased with a simultaneous increase in dosage. However, at higher pH and lower dosage, the change in TDS reduction was not significant. Thus, for $FeCl_3$, the optimum TDS reduction was observed at the maximum pH and minimum dosage. This might be attributed to adsorption and sweep flocculation phenomena. For $CuSO_4$+$FeCl_3$, TDS reduction increased with an increase in pH and decreased with an increase in dosage of the coagulant. Thus, in case of $CuSO_4$+$FeCl_3$, the optimal TDS reduction was perceived at high pH and low dosage. This might be due to higher sweep flocculation and moderate adsorption. This attributed again to the formation of TBCC in the case of both $CuSO_4$ and $CuSO_4$+$FeCl_3$ coagulant causing enhanced aggregation of flocs that boosted the settling of dissolved solid after adsorption and sweep flocculation.

4.3.6 Effect of coagulants on color reduction

The actual and predicted values relation analogy suggested by ANOVA for color reduction by $CuSO_4$, $FeCl_3$, and $CuSO_4$+$FeCl_3$ coagulants are shown in Fig. 4.1 (e), 4.2 (e), and 4.3 (e), respectively. The result showed that both actual and predicted values were close to each other justifying the significance of the developed model. The correlation coefficients (R^2 and R^2_{adj}) of developed model equation in case of $CuSO_4$, $FeCl_3$, and $CuSO_4$+$FeCl_3$ coagulants were found to be 0.9545, 0.9769, and 0.9878, and0.9219, 0.9604, and 0.9791 respectively. This proposed a reliable relation between the dependent and independent variables. The quadratic response between independent and dependent variables for color reduction is presented in Table 4.7. For color reduction, in case of $CuSO_4$, the negative impact was shown by AB while the positive impact was shown by A, B, A^2 and B^2. In case of $FeCl_3$, the negative impact was shown by A and B while a positive impact was shown by AB, A^2 and B^2. Similarly, in case of $CuSO_4$+$FeCl_3$, the negative impact was shown by A and A^2 while a positive impact was shown by B, AB, and B^2. In addition, the statistical fitness of the developed model for a response (color reduction) for all three coagulants was also examined by p-value, F value, AP, and CV. The results are presented in Table 4.7. Results show that in every aspect the developed model for color reduction is reliable and significant.

The 3D plots of response color reduction for $CuSO_4$, $FeCl_3$, and $CuSO_4$+$FeCl_3$ were analyzed to investigate the coupled effect of pH and dosage on color reduction and the results are shown in Fig. 4.4 (e), 4.5 (e), and 4.6 (e), respectively. PRE contains high levels of metals, inorganic, and derived hydrocarbons. These high molecular weight compounds are responsible for the dark color of the effluent. The color reduction of PRE through coagulation and flocculation process was perceived as a result of charge neutralization, adsorption, and sweep flocculation. In the case of $CuSO_4$, color reduction increased with an increase in pH and dosage. The optimum color reduction was observed at maximum pH and dosage in the selected range. This might be attributed to adsorption and sweep flocculation. For $FeCl_3$, initially, the color reduction decreased with an increase in pH and after pH 5, the color reduction increased, while, with the increase of dosage the color reduction decreased continuously. The optimum color reduction was attained at lower and neutral pH and dosage. This revealed that color reduction was observed in a highly acidic or neutral medium as a result of the charge neutralization of $FeCl_3$. In the case of $CuSO_4$+$FeCl_3$, initially, color reduction increased to pH 7. On further increase in pH, the color reduction decreased. With an increase in dosage, initially, the color reduction decreased after that it starts increasing. The optimum color reduction was attained at a maximum dosage and nearly at neutral pH 7.

Thus color reduction of PRE was occurred due to charge neutralization, adsorption, and sweep flocculation phenomena. However, in the case of $CuSO_4$ and $CuSO_4$+$FeCl_3$, formation of TBCC abruptly reduced the color since it acts as a decolorizing agent.

4.3.7 Process optimization

Thirteen experiments for each coagulant separately have been performed according to the set of conditions provided by the design expert software as mentioned in the experimental design matrix (Table 4.6). The optimum value of independent variable for each coagulant was obtained for all five response variables for a defined range of independent variables and constraints over each response variable as mentioned in Table 4.8.

Table 4. 8 Constraints selected for the optimization of parameters by ANOVA.

Variables	**Variables selection criteria**
A: pH	In the range
B: Dosage	In the range
Final pH	In the range
COD reduction (%)	Maximize
Turbidity reduction (%)	Maximize
TDS reduction (%)	Maximize
Color reduction (%)	Maximize

The optimum conditions for all three coagulants considering all the response variables in their predefined goal (Table 4.7) simultaneously are presented in Table 4.9. It would be appropriate to mention that there might be other optimum conditions if we consider one response variable at a time. However, in the present chapter, all five response variables are considered at the same time to determine the optimum value of an independent variable. The optimum condition for $CuSO_4$ was found to be dosage 0.74 g/L and pH 11, and for $FeCl_3$ it was dosage 0.20 g/L and pH 7, respectively. The optimum condition for $CuSO_4$+ $FeCl_3$ was found to be dosage 0.20 g/L and pH 7.1. In addition, for the validation of optimum condition obtained by ANOVA, the experiments were performed at the same optimum conditions and it was found that in each case the error was less than 3 % (Table 4.9). This clearly revealed that the model developed for coagulation and flocculation was in good agreement with the experimental results.

Table 4. 9 Comparison between actual and predicted response at optimum condition.

Conditions	**Response**					
	Final pH	**COD reduction%**	**Turbidity reduction %**	**TDS reduction %**	**Color reduction %**	**Desirability**
$CuSO_4$ (0.74 g/L at 11 pH)						
Experimental	8.690	55	97.8	92.2	94	-
Predicted response	8.466	55.932	97.050	92.286	94.204	0.876
Error	0.224	-0.932	0.75	-0.086	-0.204	-
$FeCl_3$ (0.20 g/L at 7 pH)						
Experimental	3.7	52	80	95.5	92	-
Predicted response	3.721	53.992	79.352	93.685	92.311	0.877
Error	-0.021	-1.992	0.648	1.815	-0.311	-
$CuSO_4$+ $FeCl_3$ (0.20 g/L at 7.122 pH)						
Experimental	5.1	81	93	95	95.2	-
Predicted response	5.0	76.779	89.475	94.167	95.297	0.803
Error	0	4.221	3.525	0.833	-0.097	-

4.3.8 Significance of G value

The ratio of the value of G was calculated to understand the settling velocity gradient parameters in conversion of RPM. The calculated value of G_r was 17.189, which signifies that in the flocculation process settling of particles at 200 RPM was 17.189 times more than at 30 RPM. Consequently, there should be better removal at 200 RPM, however, at very high RPM, the coagulated flocs may break and become waterborne [23]. Consequently, coagulation was performed at 200 RPM, and the flocculation of particles was performed at low RPM such as 30.

4.3.9 Characteristics of coagulation flocs formed by XPS, SEM and EDX

4.3.9.1 XPS analysis of flocs

XPS analysis was employed to examine the chemical shift of the elements from its initial state to the final state after the coagulation and flocculation process. The present chapter, mainly focused on the final elemental state of cupper and iron to understand the mechanism in case of all three coagulants and especially, the formation of TBCC in case of $CuSO_4$ and $CuSO_4$+ $FeCl_3$. Fig 4.7 (a-c) represents the XPS survey of flocs obtained after coagulation and flocculation using $CuSO_4$, $FeCl_{3,}$ and $CuSO_4$+ $FeCl_3$, respectively. The presence of Cu2p3, Fe2p, Cl2p, O1s, and S2p elements can be seen in the flocs. Fig 4.8 (a-b) displays the Cu2p3 and Fe2p XPS core-level spectra of flocs after coagulation and flocculation. The binding energy of pure Cu(I), Cu(II), and Cu(II) carbonate hydroxide were 933, 933.5, and 934.7 eV [158]. After coagulation, the binding energy of Cu2p3, shifted to 935.17 eV for $CuSO_4$, while, 935.56 eV for $CuSO_4$+ $FeCl_3$ (Fig. 4.8a). This attributes the presence of an additional component of high electron affinity, which decreased the electron density near Cu, as a result, binding energy increases. The O1s pure binding energy for O^{-1} was 529-530 eV and for O^{-2}, it was 532.6 eV [159]. In Fig 4.7 (a) and (c), the binding energy of O1s was 532.47 eV, which was nearly equal to O^{-2}. This attributes that O1s was attached with the an element of higher electron affinity than the O-H bond [160, 161]. This may reveal that the chain structure of TBCC was formed during the process. The Cl2p spectrum in Fig 4.7 (a) and (c) also confirm the chemical shift with binding energy 199.96 eV, whereas the binding energy of Cl in case of NaCl formation was 198.5-199 eV [162]. Consequently, Cu, Cl, and O confirm the existence of heavy molecular compounds present in flocs formed.

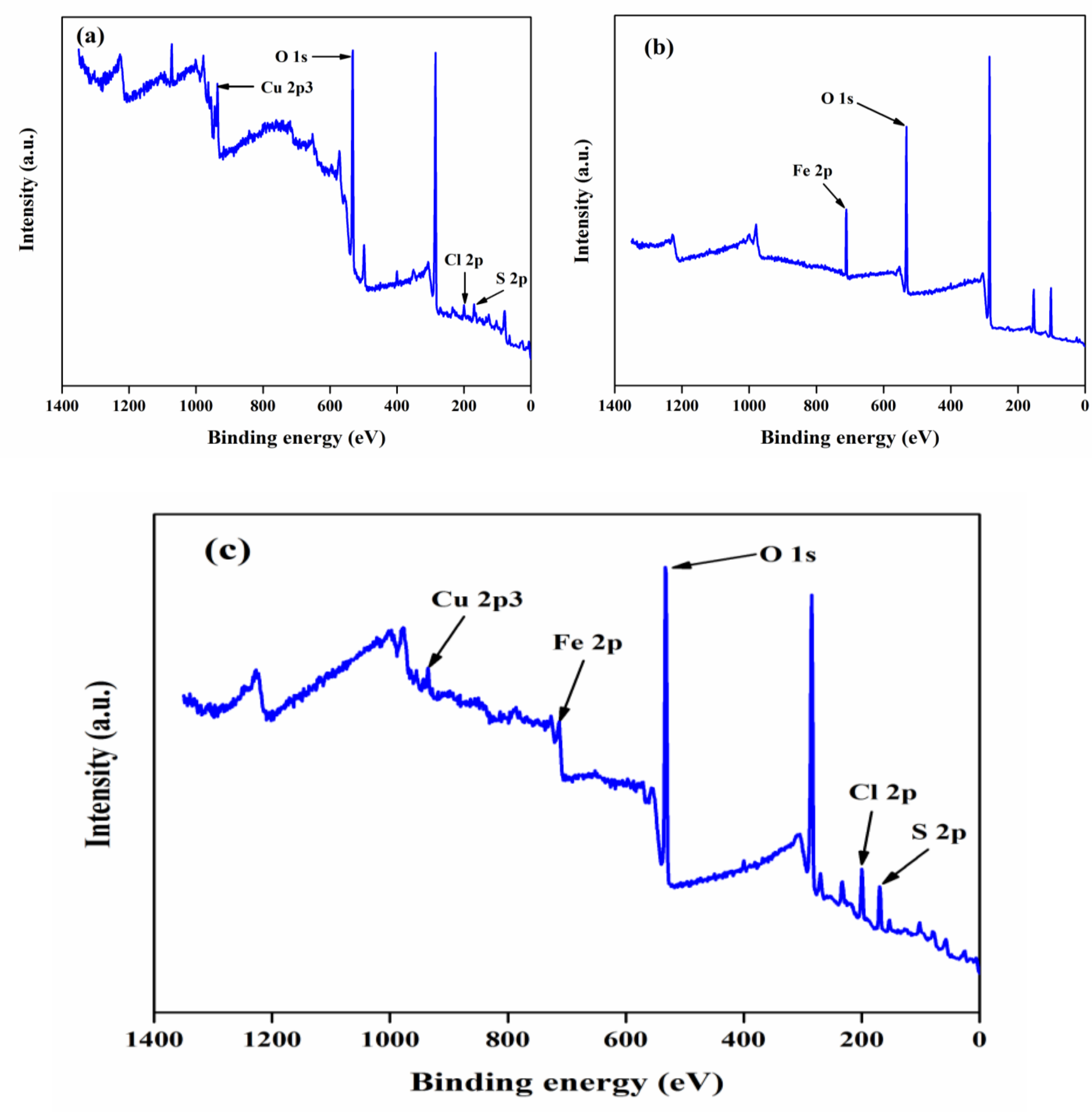

Figure 4. 7 XPS survey of flocs obtained after coagulation and flocculation using (a) $CuSO_4$ (b) $FeCl_3$ (c) $CuSO_4$+ $FeCl_3$

The Fe2p spectrum was studied for $FeCl_3$ and $CuSO_4$+ $FeCl_3$ coagulant and results are presented in Fig. 4.8b. The Fe(II) cation exhibits the pure binding energy peak at 709.8 for Fe-O bond [163]. After coagulation, the binding energy of Fe2p, shifted to 711.3 eV for $FeCl_3$, while, 713.1 eV for $CuSO_4$+ $FeCl_3$ (Fig. 4.8b). The Fe(III) cation exhibits the binding energy 711.3 eV [164]. This attributed that, the Fe exists in Fe(III) state as presented in Eq (5) and the charge neutralization phenomena were dominated for the coagulation and flocculation process. In the case of $CuSO_4$+ $FeCl_3$ coagulant, the binding energy of Fe2P was more than the Fe(III) state. This indicated the formation of $Fe_2(SO_4)_3$ as mentioned in Eq. (6).

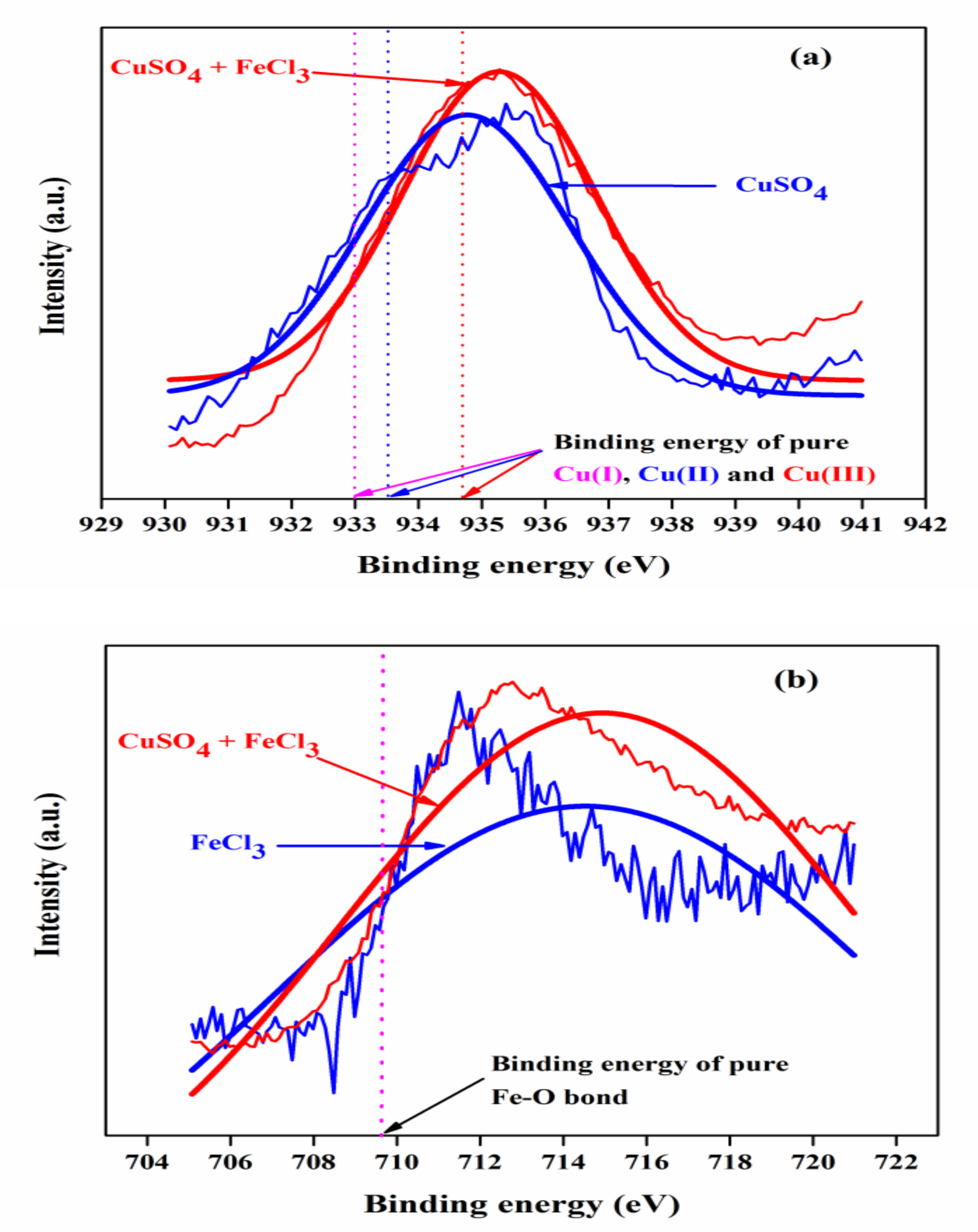

Figure 4. 8 (a) Cu2p3 (b) Fe2p XPS core level spectra of flocs in after coagulation and flocculation using $CuSO_4$, $FeCl_3$ and $CuSO_4$+ $FeCl_3$

4.3.9.2 SEM and EDX analysis of flocs

The results of SEM-EDX analysis of flocs formed during coagulation and flocculation are shown in Fig. 4.9 (a-d). The relative abundance of elements existing on the surface of the flocs formed is presented in Table 4.10. Based on the SEM microphotograph, the particles of PRE formed regular, loose, and tiny particles of identical shape and size as shown in Fig. 4.9 (a). The SEM image of $CuSO_4$ and $CuSO_4$+ $FeCl_3$ is presented in Fig. 4.9(b) and 4.9(d).

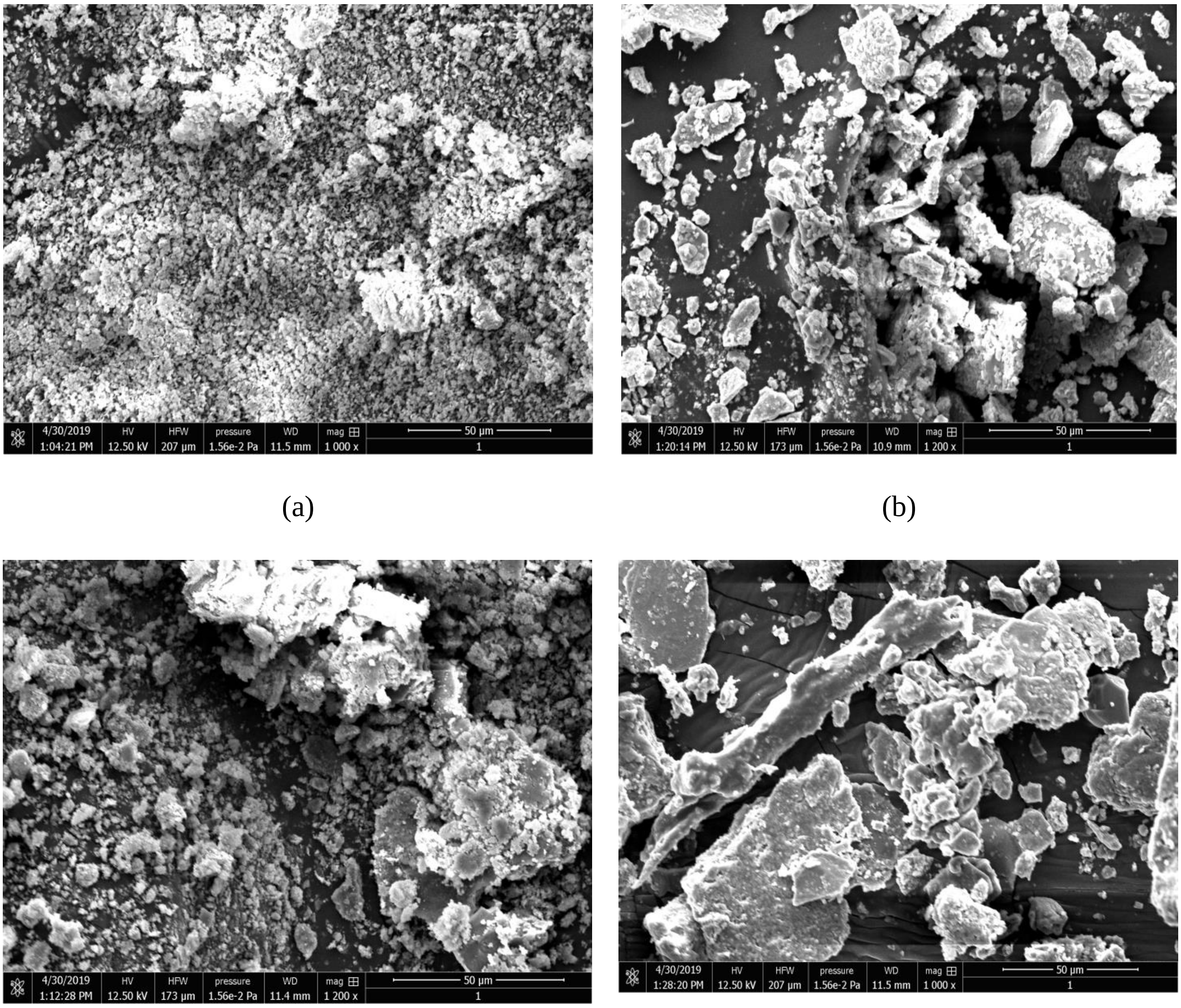

(a) (b)

(c) (d)

Figure 4. 9 SEM image of flocs formed after coagulation and flocculation (a) PRE (b) $CuSO_4$ (c) $FeCl_3$ (d) $CuSO_4$+ $FeCl_3$ coagulants

Table 4. 10 EDX analysis of the flocs formed during coagulation and flocculation of the PRE using $CuSO_4$, $FeCl_3$, and $CuSO_4$+ $FeCl_3$ coagulants

S.NO.	Element	PRE (%)	$CuSO_4$ (%)	$FeCl_3$ (%)	$CuSO_4$+ $FeCl_3$ (%)
1.	Carbon	19	10	18	13
2.	Nitrogen	1	1	1	1
3.	Oxygen	20	24	19	21
4.	Copper	1	25	1	11
5.	Sodium	2	10	3	12
6.	Magnesium	4	1	2	3
7.	Aluminium	8	1	2	7
8.	Sulphur	10	9	7	7
9.	Lead	13	9	7	6
10.	Silver	2	2	2	2
11.	Potassium	3	1	2	3
12.	Vanadium	2	1	1	2
13.	Chromium	1	1	1	1
14.	Manganese	1	1	1	1
15.	Iron	10	1	32	8
16.	Nickel	1	1	1	1
17.	Zinc	1	1	0	1
18.	Arsenic	1	1	0	0

In both cases, the compact, clustered, and large size crystal-like structure of flocs can be seen, however, in case of $CuSO_4$+ $FeCl_3$, the size of crystal are even larger as compare to $CuSO_4$. This attributes that adsorption phenomena, inter-particle bridging, and formation of TBCC octahedral crystallites [165, 166] are dominant in case of $CuSO_4$+ $FeCl_3$ as compare to $CuSO_4$. However, in case of $FeCl_3$ coagulant, the irregular granular units of small size can be been seen in Fig. 4.9(c). This attributes that small size flocs are settled and the charge neutralization phenomena are dominant in the case of $FeCl_3$. Based on EDX analysis, 18 elements were detected in which carbon, oxygen, copper, iron, sulphur, and lead were found in a higher percentage for all three types of flocs (Table 4.10). The detection of carbon on the surface of sludge is attributed to COD reduction capacity of sludge [88]. Maximum carbon was found in case of $CuSO_4$+ $FeCl_3$ coagulant at its optimum condition. This result is well supported by the efficiency of $CuSO_4$+ $FeCl_3$ coagulant for a reduction in the percentage of all selected dependent variables.

4.4 Conclusion

The wastewater collected from the effluent treatment plant of petroleum refinery was treated using coagulation and flocculation process (Jar test method). The copper and iron-based coagulants i.e. $CuSO_4$, $FeCl_3$, and $CuSO_4$+$FeCl_3$ (1:1 ratio mixture) were used for the process. The independent process parameters such as pH and coagulant dosage were optimized using response surface methodology with central composite design technique considering final pH, reduction in COD, turbidity, TDS, and color as dependent variables. The optimum condition for $CuSO_4$ was found as dosage 0.74 g/L and pH 11, with the final pH of 8.46. The reduction in COD, turbidity, TDS, and color was as 55.93, 97.05, 92.28, and 94.20 %, respectively. For $FeCl_3$, the optimum condition was dosage 0.20 g/L and pH 7.0, with final pH of 3.72 and reduction in COD, turbidity, TDS and color were 53.99, 79.35, 93.68, and 92.31%, respectively. In case of $CuSO_4$+ $FeCl_3$, the optimum dosage was found to be 0.20 g/L and pH 7.10, with a final pH of 5.0. The corresponding reduction in COD, turbidity, TDS, and color were 76.77, 89.47, 94.16, 95.29%, respectively. The mixed coagulant $CuSO_4$+$FeCl_3$ showed better results for all the dependent variables as compared to the individual $CuSO_4$ and $FeCl_3$ coagulants. The mixed coagulant $CuSO_4$+$FeCl_3$, along with adsorption and sweep flocculation, the formation of tribasic copper chloride (TBCC) was prominent. The TBCC acts as a proceeding intermediate in the pH ranging from 5 to 7. TBCC formation enhanced the flocculation process by its catalytic, decolorizing, and octahedral structural properties. $CuSO_4$ coagulant in presence of chloride ions and alkali also form TBCC. The final pH of solution at the optimum condition for all three coagulants is under the disposal limit. The analysis of SEM, EDX, and XPS indicates the formation of TBCC which helped in enhancing the ability of coagulation and flocculation.

It may be concluded that mixed coagulant ($CuSO_4$+$FeCl_3$) is well suited for the treatment of PRE using coagulation and flocculation process. The optimization of the process parameters may increase the process efficiency and reduction in COD, turbidity, TDS, and color may enhance the efficiency of secondary treatment of wastewater.